

Analysis of Distributed Thermopiezoelectric Sensors and Actuators in Advanced Intelligent Structures

S. S. Rao* and M. Sunar†

Purdue University, West Lafayette, Indiana 47907

The quasistatic equations of piezoelectricity and thermopiezoelectricity are used to develop a finite element formulation of distributed piezoelectric and thermopiezoelectric media. The formulation is then integrated with the distributed sensing and control of advanced intelligent structure design. The procedure is illustrated with the help of two example problems. The purpose of the first example, which consists of two piezoelectric layers used as a bimorph robotic finger, is to check the accuracy of the finite element solution with the analytical one. As a second example, an aluminum beam is utilized along with two polyvinylidene fluoride layers acting as distributed actuator and sensor to study the distributed control of the beam when thermal effects are present. It is concluded that the thermal effects are important in the precision distributed control of intelligent structures.

Nomenclature

A	= system matrix
B	= input matrix
C	= constant gain matrix
$C_{\theta u}$	= thermal expansion rate matrix
$C_{\theta \phi}$	= pyroelectric rate matrix
$C_{\theta \theta}$	= heat conduction rate matrix
c	= matrix of elastic stiffness coefficients
c_p	= capacitance
D	= electric displacement vector
E	= electric field vector
e	= matrix of piezoelectric coefficients
F	= global mechanical force (disturbance) vector
F_G	= global feedback force
F_Q	= global heat force (disturbance) vector
G	= global feedback charge vector
h	= vector of heat flux
K	= matrix of heat conduction coefficients
K_{uu}	= elastic stiffness matrix
$K_{u\theta}$	= thermal expansion stiffness matrix
$K_{u\phi}$	= piezoelectric stiffness matrix
$K_{\phi\phi}$	= dielectric stiffness matrix
$K_{\phi\theta}$	= pyroelectric stiffness matrix
$K_{\theta\theta}$	= heat conduction stiffness matrix
N_u	= displacement shape function matrix
N_ϕ	= electrical shape function matrix
N_θ	= thermal shape function matrix
P	= vector of pyroelectric coefficients
Q	= global external heat vector
Q_i	= heat generated at the i th node
R	= resistance coefficient
S	= strain vector
T	= stress vector
u	= global displacement vector
u_G	= control input vector
V	= global feedback voltage vector
V_i	= feedback voltage applied to the i th node
W	= heat source intensity per unit volume per unit time
x	= state vector
α	= scalar of constitutive coefficients
ϵ	= matrix of dielectric coefficients

η	= entropy per unit volume
Θ	= absolute temperature
θ	= global temperature variation vector
θ_0	= reference temperature
λ	= vector of thermal expansion coefficients
ρ	= mass density of piezoelectric material
ϕ	= global electric potential vector
$()^T$	= transpose of $()$
$()$	= $(\partial/\partial t)()$
$()$	= $(\partial^2/\partial t^2)()$

I. Introduction

WITH increasing space activity, the use of controlled light flexible structures has become the subject of focus in recent years. The rapid developments in space exploration have reached a level that calls for a departure from the conventional control approaches to satisfy the stringent system performance requirements set forth for space structures.

Because of their self-monitoring and self-adaptive capabilities, the so-called advanced intelligent structures have attracted considerable research over the past few years. Such structures contain highly integrated or hierarchic control architecture. These intelligent structures have some distinct advantages over conventional actively controlled structures. Since the intelligent structures are distributed (instead of being discrete) in nature, more accurate response monitoring and control are possible.

There are two basic phenomena, characteristic of piezoelectric materials, which permit them to be used as sensors and actuators in a control system. The first phenomenon is called the direct piezoelectric effect that implies that when some mechanical force or pressure is applied on a piezoelectric component, some electrical charge or voltage is induced in the piezoelectric material. Conversely, if some charge or voltage is imposed on a piezoelectric material, the material reacts by generating some mechanical force and strain. This phenomenon is called the converse piezoelectric effect. These direct and converse piezoelectric effects form a basis in the use of a piezoelectric material as a sensor and actuator, respectively. The direct piezoelectric effect was first discovered by the Curie brothers in 1880.¹

Although piezoelectricity has a long history, its use in control applications is relatively new. Because of their distinct properties, the piezoelectric materials are ideally suited for use in the vibration control of distributed systems. The use of piezoelectric materials as actuators in adaptive structures was discussed by Forward,² Bailey and Hubbard,³ and Hagood et al.⁴ The implementation of distributed control systems by piezoelectric materials was examined by Hanagud et al.,⁵ Crawley and de Luis,⁶ and Cudney et al.⁷ The analytical investigation of piezoelectric actuators bonded to the surface of elastic distributed structures was carried out by Dim-

Received March 10, 1992; revision received Oct. 24, 1992; accepted for publication Oct. 29, 1992. Copyright © 1992 by S. S. Rao and M. Sunar. Published by the American Institute of Aeronautics and Astronautics, Inc., with permission.

*Professor, School of Mechanical Engineering.

†Graduate Assistant, School of Mechanical Engineering.

itridis et al.⁸ The endpoint position control of a robotic flexible arm driven by piezoelectric bimorph cells was presented by Jiang et al.⁹ Polyvinylidene fluoride (PVDF) is a piezoelectric film that was originally discovered by Kawai in 1969¹⁰ and has some advantages over piezoceramics and other piezoelectric crystals. The application of PVDF to vibration suppression was investigated by Plump et al.¹¹ Most of the piezoelectric studies are theoretical and experimental, and modeling of the piezoelectric media by the finite element method (FEM) is limited.^{12,13} A distributed piezoelectric sensor/actuator design, based on a FEM model, was developed and applied in the vibration control of a plate by Tzou and Tseng.¹⁴

It has long been recognized that mechanical, electrical, and thermal fields are coupled in most of the physical problems. Because of their inherent complexity, relatively few solutions to such coupled problems are available in the literature. The governing equations of a thermopiezoelectric medium, where deformation, temperature, and electric fields are coupled, were first derived by Mindlin.¹⁵ A system of two-dimensional equations for high-frequency motions of thermopiezoelectric crystal plates was obtained by Mindlin.¹⁶ Some general theorems of thermopiezoelectricity were given and the generalized Hamilton principle was deduced by Nowacki.¹⁷ Uniqueness and reciprocity theorems for quasistatic and dynamic thermopiezoelectricity were given by Iesan.¹⁸

Although thermopiezoelectricity has been studied and its theory has been established for the last two decades, most of the investigations have been confined to theoretical studies. The application of thermopiezoelectricity theory to practical engineering and physical problems in general, and vibration control of advanced intelligent structures in particular, is virtually absent in the literature. It has been recognized that the temperature variation in the piezoelectric polymer (PVDF) can affect the overall performance of a distributed control system.¹⁴ It has also been recognized that these composite materials have different response characteristics at different temperatures,¹⁹ and as a result, in some cases, it may be impossible to accurately design sensors and actuators for a distributed control system without considering the thermal effects. Thermal effects are especially important for some piezoelectric materials, and PVDF is reported to have a strong pyroelectric response.²⁰ Hence, it may be crucial to include the thermal effects in the distributed sensing and control of advanced intelligent structures.

Thermal effects in a distributed control system become important when the system has to operate in a high- or low-temperature environment. Such environments are quite possible in the space applications of intelligent structures. The thermal modeling of distributed control systems is also applicable to flexible robotic manipulators used in adverse environments, such as cleaning of boilers and nuclear power reactors. Even when thermal effects of the environment are negligible, the applied feedback voltage acts as a thermal disturbance as the voltage increases. Thermal effects of the feedback voltage are expected to have more significance in the future, since the control applications demand more power with the ascending performance requirements.

The FEM has been established as a powerful numerical technique that provides solutions to many complicated engineering problems and is widely used in modern engineering designs and analyses. Modeling of the thermopiezoelectric effect by the FEM and its implementation into distributed sensing and control problems appears to be lacking in the literature. Owing to difficulty associated with finding analytical solutions to thermopiezoelectric problems, modeling of such problems by the FEM becomes very important.

In this work, the FEM formulation of thermopiezoelectric problems is presented, and its application to distributed dynamic measurement and active vibration control of advanced intelligent structures is studied. It is concluded that the inclusion of thermal effects in a distributed control system will help the performance characteristics of the system to improve and also to gain a better insight into the thermopiezoelectric phenomenon. The proposed method is quite general and is expected to be useful for flexible space structures as well as flexible robotic manipulators operating in environments where the thermal effects are important.

II. Finite Element Formulation of Thermopiezoelectric Problems

Linear Thermopiezoelectricity

The governing equations for quasistatic thermopiezoelectricity are given by¹⁶

$$\begin{aligned} T &= cS - eE - \lambda\theta \\ D &= e^T S + \varepsilon E + P\theta \\ \eta &= \lambda^T S + P^T E + \alpha\theta \end{aligned} \quad (1)$$

The following relations are also noted¹⁶

$$h = -K \nabla \theta, \quad E = -\nabla \phi \quad (2)$$

Finite Element Formulation of Heat Equation

The generalized heat equation is given by¹⁷

$$\Theta \eta = -\nabla^T h + W \quad (3)$$

where $\Theta = \theta_0 + \theta$. By using Eqs. (2) and (3), in conjunction with the divergence theorem, the finite element approximation of the heat equation can be obtained as (after assemblage)

$$-C_{\theta u} \dot{u} + C_{\theta \phi} \dot{\phi} - C_{\theta \theta} \dot{\theta} - K_{\theta \theta} \theta = Q \quad (4)$$

The element matrices and external heat vector are given by

$$\begin{aligned} C_{\theta ui} &= \int_{V_i} \theta_0 N_i^T \lambda^T B_u \, dV_i \\ C_{\theta \phi i} &= \int_{V_i} \theta_0 N_i^T P^T B_\phi \, dV_i \\ C_{\theta \theta i} &= \int_{V_i} \theta_0 N_i^T \alpha N_i \, dV_i \\ K_{\theta \theta i} &= \int_{V_i} B_i^T K^T B_i \, dV_i \end{aligned} \quad (5)$$

$$Q_i = \int_{A_i} N_i h^T n \, dA_i - \int_{V_i} W N_i^T \, dV_i$$

where V_i is the volume of the element considered, A_i is the element area whose normal vector is n , and $B_u = L_u N_u$ with L_u denoting a differential operator matrix. Note that the subscripts denote the fields (i.e., u denotes the mechanical field, ϕ the electric field, and θ the thermal field). For an isentropic process for which $\eta = 0$, Eq. (4) reduces to

$$-K_{\theta \theta} \theta = Q \quad (6)$$

Finite Element Formulation of Actuator and Sensor Equations

A functional Π is defined as

$$\begin{aligned} \Pi &= \int_V (G + \eta \Theta) \, dV - \int_V u^T P_b \, dV \\ &\quad - \int_{S_1} u^T P_s \, dS - u^T P_c + \int_{S_2} \phi \sigma \, dS \end{aligned} \quad (7)$$

where G is the thermodynamic potential, P_b the vector of body forces applied to volume V , P_s the vector of surface forces applied to surface S_1 , P_c the vector of concentrated forces, and σ the surface charge on the surface S_2 . The Hamilton's principle can be expressed as

$$\delta \int_{t_1}^{t_2} (K_i - \Pi) \, dt = 0 \quad (8)$$

where Ki represents the kinetic energy given by

$$Ki = 1/2 \int_V \rho \dot{u}^T \dot{u} dV \quad (9)$$

which yields

$$\begin{aligned} \int_{t_1}^{t_2} \delta Ki dt &= \int_{t_1}^{t_2} \int_V \rho \delta \dot{u}^T \dot{u} dt dV \\ &= - \int_{t_1}^{t_2} \int_V \rho \delta u^T \ddot{u} dt dV \end{aligned} \quad (10)$$

on using integration by parts along with proper boundary conditions. Furthermore,

$$\delta G = \delta S^T T - \delta E^T D - \delta \theta \eta \quad (11)$$

Using Eqs. (11) and (12), and substituting for T and D from the governing equations, the following actuator and sensor equations can be obtained (after assemblage):

$$\begin{aligned} M_{uu} \ddot{u} + K_{uu} u + K_{u\phi} \phi - K_{u\theta} \theta &= F \\ K_{\phi u} u - K_{\phi\phi} \phi + K_{\phi\theta} \theta &= G \end{aligned} \quad (12)$$

The element matrices and vectors are given by

$$\begin{aligned} M_{uu} &= \int_{V_i} \rho N_u^T N_u dV_i, & K_{uu} &= \int_{V_i} B_u^T C B_u dV_i \\ K_{u\phi} &= \int_{V_i} B_u^T e B_\phi dV_i, & K_{u\theta} &= \int_{V_i} B_u^T \lambda N_\theta dV_i \\ K_{\phi u} &= \int_{V_i} B_\phi^T e^T B_u dV_i, & K_{\phi\phi} &= \int_{V_i} B_\phi^T \epsilon B_\phi dV_i \\ K_{\phi\theta} &= \int_{V_i} B_\phi^T P N_\theta dV_i, & G_i &= - \int_{S_{2i}} N_\theta^T \sigma dS_i \\ F_i &= \int_{V_i} N_u^T P_b dV_i + \int_{S_{1i}} N_u^T P_s dS_i + N_u^T P_c \end{aligned} \quad (13)$$

If the thermal effects are not considered, Eqs. (12) reduce to the following form

$$\begin{aligned} M_{uu} \ddot{u} + K_{uu} u + K_{u\phi} \phi &= F \\ K_{\phi u} u - K_{\phi\phi} \phi &= G \end{aligned} \quad (14)$$

The heat, actuator, and sensor equations, Eqs. (4) and (12), can be collectively written as

$$\begin{aligned} \begin{bmatrix} M_{uu} & 0 & 0 \\ 0 & 0 & 0 \\ 0 & 0 & 0 \end{bmatrix} \begin{Bmatrix} \ddot{u} \\ \ddot{\phi} \\ \ddot{\theta} \end{Bmatrix} + \begin{bmatrix} 0 & 0 & 0 \\ 0 & 0 & 0 \\ -C_{\theta u} & C_{\theta\phi} & -C_{\theta\theta} \end{bmatrix} \begin{Bmatrix} \dot{u} \\ \dot{\phi} \\ \dot{\theta} \end{Bmatrix} \\ + \begin{bmatrix} K_{uu} & K_{u\phi} & -K_{u\theta} \\ K_{\phi u} & -K_{\phi\phi} & K_{\phi\theta} \\ 0 & 0 & -K_{\theta\theta} \end{bmatrix} \begin{Bmatrix} u \\ \phi \\ \theta \end{Bmatrix} = \begin{Bmatrix} F \\ G \\ Q \end{Bmatrix} \end{aligned} \quad (15)$$

The heat generation in a distributed control system may be due to the high voltage applied to the piezoelectric actuator and/or the high- or low-temperature environment in which the control system

is to operate. In either case, Eqs. (15) can be used to study the thermal effects on the distributed control system.

III. Distributed Dynamic Measurement and Active Vibration Control of Intelligent Structures

The intelligent structure of interest here is composed of a beam placed between two thin piezoelectric layers functioning as the distributed sensor and actuator. This configuration is illustrated in Fig. 1 where the bottom piezoelectric layer acts as a distributed sensor and the top one as a distributed actuator. The oscillation of the beam induces a voltage across the piezoelectric sensor. This voltage is then fed back to the piezoelectric actuator according to the control law implemented. The feedback voltage causes a strain in the actuator that, in turn, generates a moment to counteract the motion of the beam.

Consideration of the Feedback Voltage as a Heat Source

If the thermal effects are not considered, Eqs. (14) can be used to find the voltage fed back to the actuator layer. The sensor output can be found using the second of Eqs. (14) as

$$\phi = K_{\phi\phi}^{-1} K_{\phi u} u \quad (16)$$

where it is assumed that the applied charge G is zero in the sensor layer. Note that in Eq. (16), $K_{\phi\phi}^{-1}$ is a well-conditioned matrix for proper electrical boundary conditions. For matrices of large size, any suitable numerical technique can be used for the inversion. When the Guyan reduction method²¹ is applied to Eqs. (14), the equations are reduced to one equation as follows:

$$M_{uu} \ddot{u} + (K_{uu} + K_{u\phi} K_{\phi\phi}^{-1} K_{\phi u}) u = F + F_G \quad (17)$$

where the feedback force F_G is given by

$$F_G = K_{u\phi} K_{\phi\phi}^{-1} G \quad (18)$$

The control law on G is implemented as

$$G = -C\dot{\phi} = -CK_{\phi\phi}^{-1} K_{\phi u} \dot{u} \quad (19)$$

where the sensor output ϕ is substituted from Eq. (16). Substituting Eq. (19) into Eq. (18) yields

$$F_G = -K_{u\phi} K_{\phi\phi}^{-1} CK_{\phi\phi}^{-1} K_{\phi u} \dot{u} \quad (20)$$

Substituting Eq. (20) into Eq. (17) and rearranging it gives

$$\begin{aligned} M_{uu} \ddot{u} + K_{u\phi} K_{\phi\phi}^{-1} CK_{\phi\phi}^{-1} K_{\phi u} \dot{u} \\ + (K_{uu} + K_{u\phi} K_{\phi\phi}^{-1} K_{\phi u}) u = F \end{aligned} \quad (21)$$

When the thermal effects of the feedback voltage are considered, it is assumed that the piezoelectric actuator reacts to the feedback voltage as a resistive element, and hence the heat generated in the i th node of the actuator can be approximated using a Taylor's series expansion as

$$Q_i = \frac{V_i^2}{R} \approx \frac{2V_{i0}V_i - V_{i0}^2}{R} \quad (22)$$

where V_{i0} represents the feedback voltages applied to the i th node of the actuator. When the Guyan reduction method is applied to Eqs. (15), the following equation is obtained

$$M_{uu} \ddot{u} + (K_{uu} + K_{u\phi} K_{\phi\phi}^{-1} K_{\phi u}) u = F + F_G \quad (23)$$

where the feedback force F_G is taken as

$$F_G = K_{u\phi} K_{\phi\phi}^{-1} G + (K_{u\phi} K_{\phi\phi}^{-1} K_{\phi\theta} - K_{u\theta}) K_{\theta\theta}^{-1} Q \quad (24)$$

where $K_{\theta\theta}^{-1}$ is a well-defined matrix for proper thermal boundary conditions. The relation between the feedback voltage V and charge G is given by

$$G = c_p V \quad (25)$$

where c_p is the capacitance of the piezoelectric actuator. Using Eqs. (19), (24), and (25) yields the feedback force F_G as

$$F_G = - \left\{ K_{u\phi} K_{\phi\phi}^{-1} + \frac{2}{c_p R} (K_{u\phi} K_{\phi\phi}^{-1} K_{\phi\theta} - K_{u\theta}) K_{\theta\theta}^{-1} [V_0] \right\} \times C K_{\phi\phi}^{-1} K_{\phi\theta} \dot{u} \quad (26)$$

where $[V_0]$ is a diagonal matrix whose i th diagonal element is V_{i0} . Note the difference between Eqs. (20) and (26). Because Eq. (26) introduces damping into the control system whose equation is given by Eq. (23), the heating induced by the feedback voltage will affect the damping ratio of the system.

Consideration of an Independent Heat Source

In this case, no relation exists between the heat source (or sink) and the feedback voltage. The equations of motion of the dynamic system can be written in standard state-space form as

$$\dot{x} = A x + B u_G \quad (27)$$

Equations (15) can be expressed in the state-space form of Eq. (27) with

$$x = \begin{Bmatrix} \theta \\ u \\ \dot{u} \end{Bmatrix}, \quad u_G = \{V\} = \frac{1}{c_p} \{G\} \quad (28)$$

$$A = \begin{bmatrix} C_2^{-1} K_{\theta\theta} & 0 & -C_2^{-1} C_1 \\ 0 & 0 & I \\ M_{uu}^{-1} K_2 & -M_{uu}^{-1} K_1 & 0 \end{bmatrix}, \quad B = \begin{bmatrix} 0 \\ 0 \\ M_{uu}^{-1} D \end{bmatrix}$$

where

$$K_1 = K_{uu} + K_{u\phi} K_{\phi\phi}^{-1} K_{\phi u}, \quad K_2 = K_{u\theta} - K_{u\phi} K_{\phi\phi}^{-1} K_{\phi\theta} \quad (29)$$

$$D = K_{u\phi} K_{\phi\phi}^{-1}$$

$$C_1 = -C_{\theta u} + C_{\theta\phi} K_{\phi\phi}^{-1} K_{\phi u}, \quad C_2 = -C_{\theta\theta} + C_{\theta\phi} K_{\phi\phi}^{-1} K_{\phi\theta}$$

If an isentropic process is assumed, the equations of motion can be expressed in state-space form with

$$x = \begin{Bmatrix} u \\ \dot{u} \end{Bmatrix}, \quad u_G = \{V\} \quad (30)$$

$$A = \begin{bmatrix} 0 & I \\ -M_{uu}^{-1} K_1 & 0 \end{bmatrix}, \quad B = \begin{bmatrix} 0 \\ M_{uu}^{-1} D \end{bmatrix}$$

The equations of motion, in state-space form, are used to apply the linear quadratic regulator (LQR) theory to derive the control law. The response of the closed-loop system is computed for the thermal and mechanical disturbances (Q and F) and the results are then compared to see the degree of thermal effects on the distributed control system.

IV. Numerical Study

A piezoelectric bimorph finger²² shown in Fig. 1 is considered in order to check the accuracy of the piezoelectric finite element model. Two pieces of polymeric PVDF are attached together forming a basic bimorph beam structure. The poling directions of the two layers oppose each other and hence a pure bending moment is

generated throughout the bimorph beam when an external voltage is applied. The dimensions of the finger are $L = 100$ mm and $h = 1$ mm. The finger is divided into 10 elements for the finite element model. The analytical solution to transverse displacement u is given by²²

$$u(x) = 1.5 \frac{e_{31} V}{Y} \left(\frac{x}{h} \right)^2 \quad (31)$$

where Y is the Young's modulus and V is the applied voltage. To compare the finite element solution with the analytical solution, Eq. (31), the static transverse displacement of the beam using Eqs. (14) is written as

$$[K_{uu} + K_{u\phi} K_{\phi\phi}^{-1} K_{\phi u}] u = K_{u\phi} K_{\phi\phi}^{-1} G \quad (32)$$

When a unit voltage is applied, the deflection of the beam at the nodes shown in Fig. 2 is found using Eqs. (31) and (32) and the results are shown in Fig. 3. The deflection of the beam for different values of the applied voltage is also computed for both cases as depicted in Fig. 4. The results show the close agreement between the analytical and finite element solutions.

A cantilevered beam (Fig. 5) is used as a numerical example to further implement the procedure outlined earlier. The beam is sandwiched between two PVDF layers that act as a distributed thermopiezoelectric actuator at the top and as a sensor at the bottom.

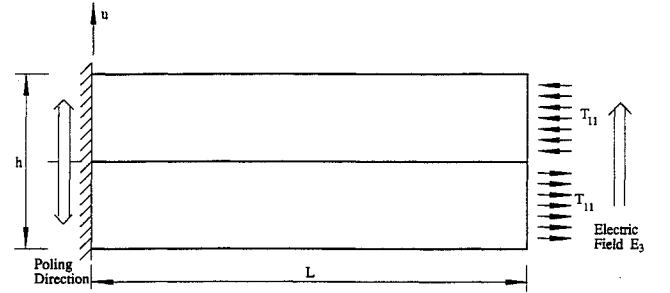


Fig. 1 Piezoelectric bimorph finger under pure bending (not to scale).

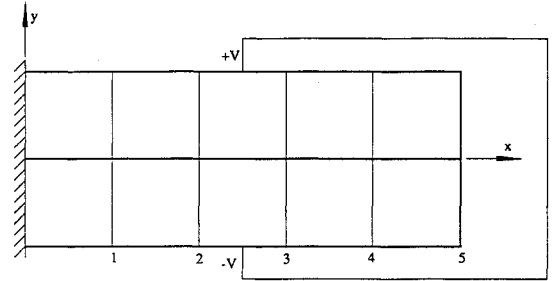


Fig. 2 Finite element modeling of the piezoelectric bimorph finger (not to scale).

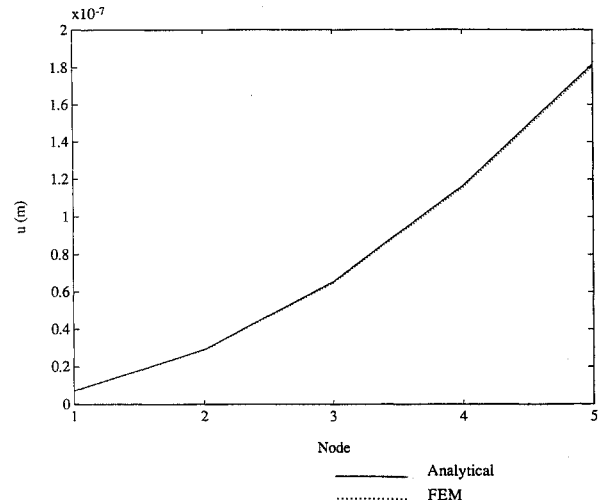


Fig. 3 Static deflection of the finger subjected to a unit voltage.

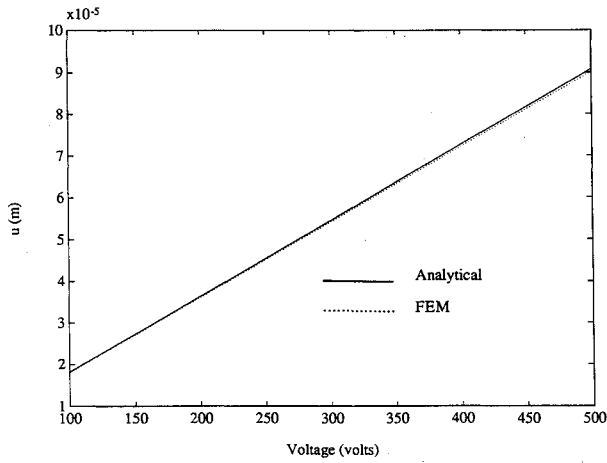


Fig. 4 Deflection of the tip of the finger vs applied voltage.

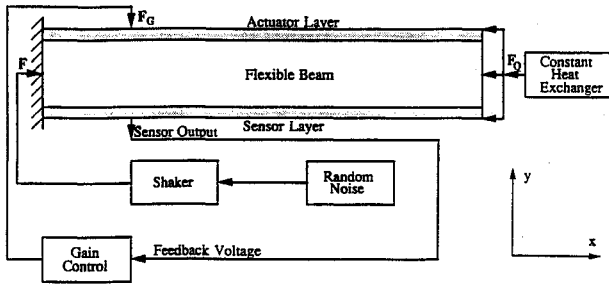


Fig. 5 Thermopiezoelectric distributed control system.

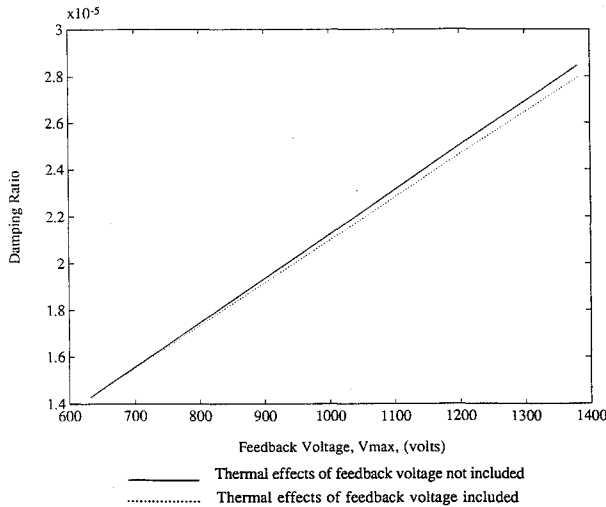


Fig. 6 Damping ratio of the closed-loop system for different values of feedback voltage.

The beam, sensor, and actuator are each divided into three elements, and hence the total number of elements of the control system is nine. The length and width of the system in respective order are 0.06 and 0.005 m. The height of the beam and PVDF is 0.005 and 0.0001 m, respectively. In Fig. 5, F_G represents the control force, and F and F_Q denote the mechanical and thermal disturbance forces, respectively. Since the thermopiezoelectric layer at the top acts as a distributed actuator and the layer at the bottom as a distributed sensor, the sensor detects the disturbance (mechanical vibration F and heating F_Q) and produces a signal. The signal is then amplified by the feedback gains and fed back to the actuator to generate a counteracting moment to control the flexible beam. The inner surfaces of the piezoelectric layers (surfaces contacting the beam) are grounded. It is assumed that the temperature changes on the inner piezoelectric surfaces are negligible when compared with those on the outer surfaces. The properties of the PVDF and beam used in the numerical study are given in Table 1 (see Refs. 14, 20, and 23–27).

When the feedback charge G alone is considered as the origin of thermal disturbance on the control system, only the tip velocity \dot{u}_T is fed back to the actuator to clearly demonstrate thermal effects of the feedback charge (voltage). After the control law is implemented the equations of motion of the system become

$$M_{uu}\ddot{u} + \left\{ K_{u\phi}K_{\phi\phi}^{-1} + \frac{2}{c_p R} (K_{u\phi}K_{\phi\phi}^{-1}K_{\phi\theta} - K_{u\theta}) K_{\theta\theta}^{-1} [V_0] \right\} \\ \times CK_{\phi\phi}^{-1}K_{\phi u}\dot{u}^* + (K_{uu} + K_{u\phi}K_{\phi\phi}^{-1}K_{\phi u})u = F \quad (33)$$

where \dot{u}^* is the velocity vector whose components, except \dot{u}_T , are set to zero. Without thermal effects Eq. (33) reduces to

$$M_{uu}\ddot{u} + K_{u\phi}K_{\phi\phi}^{-1}CK_{\phi\phi}^{-1}K_{\phi u}\dot{u}^* + (K_{uu} + K_{u\phi}K_{\phi\phi}^{-1}K_{\phi u})u = F \quad (34)$$

To see the thermal impact of the feedback charge on the damping ratio of the closed-loop system, the damping ratio of the control system for different gain constants c was calculated using Eqs. (33) and (34) as shown in Fig. 6. As can be seen from Fig. 6, the system with thermal effects caused by the feedback voltage has a lower damping ratio compared with the system without thermal effects. The damping ratio of the system increases when the feedback gain c and hence the feedback voltage increase, but this is less so when thermal effects of the feedback voltage are included. Note that Fig. 6 considers thermal effects of only the feedback voltage on the damping ratio of the closed-loop system. These thermal effects together with those coming from other environmental sources can have much greater impact in the damping ratio of the closed-loop system.

When an independent heat source (or sink) is considered for thermal effects on the distributed control system, Eqs. (25–27) are used to model the system in state-space form and to design a controller for the system using LQR theory. The response of the closed-loop system due to F (a unit step force acting in the y direc-

Table 1 Properties of materials

PVDF	300 K	350 K
c_{11} , Pa	3.8×10^9	1.8×10^9
e_{31} , C/m ²	0.046	0.049
p_3 , C/m ² K	-40×10^{-6}	-55×10^{-6}
k_{33} , W/m K	0.12	0.12
ϵ_{11} , F/m	1.026×10^{-10}	1.553×10^{-10}
ϵ_{33} , F/m	1.026×10^{-10}	1.553×10^{-10}
c_p , F	3.8×10^{-6}	3.8×10^{-6}
R , Ω	500	500
ρ , kg/m ³	1800	1800
Beam		
c_{11} (Young's modulus), Pa	7.3×10^{10}	
ρ , kg/m ³	2750	
ν (Poisson's ratio)	0.33	

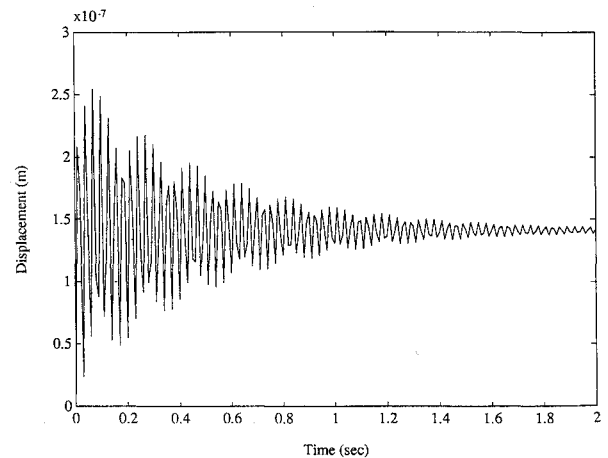
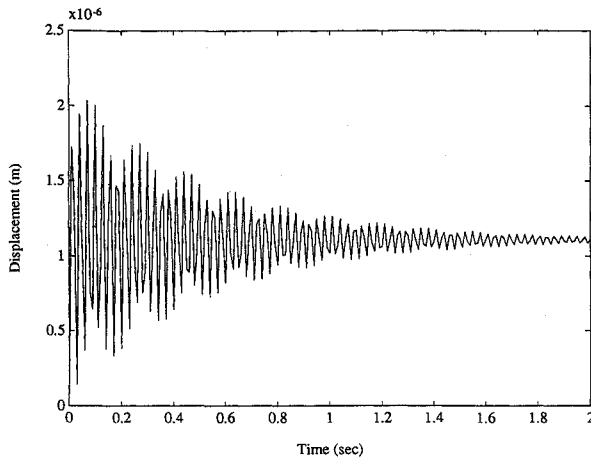
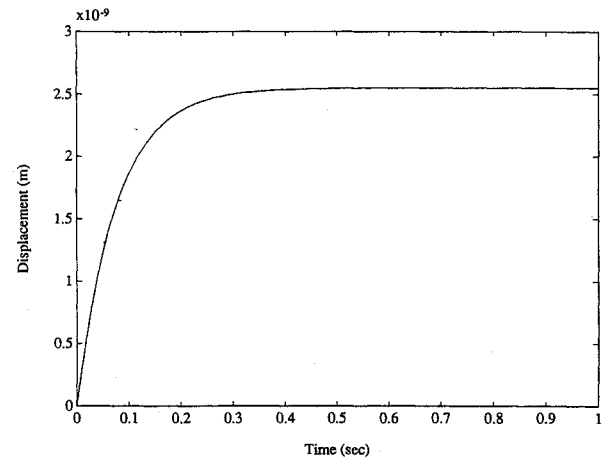
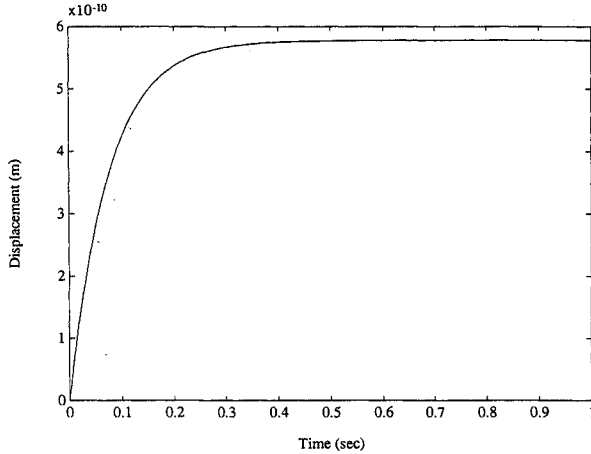
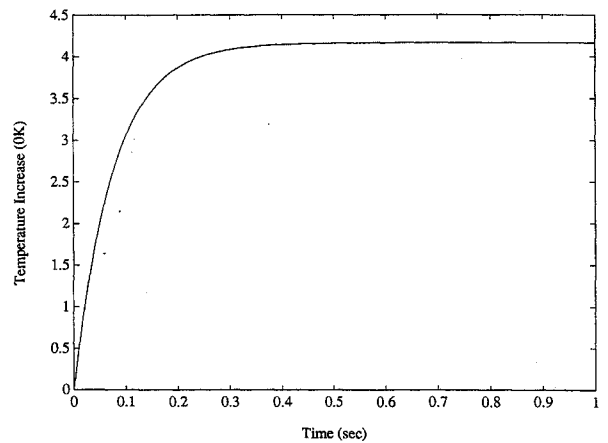


Fig. 7 Tip displacement of the beam in the x direction in response to F .


 Fig. 8 Tip displacement of the beam in the y direction in response to F .

 Fig. 10 Tip displacement of the beam in the y direction in response to F_Q .

 Fig. 9 Tip displacement of the beam in the x direction in response to F_Q .

 Fig. 11 Temperature increase of the tip of the actuator θ_1 due to Q .

tion at the tip of the beam) and F_Q (thermal force caused by a constant uniform heat flux of 5 kW/m^2 in z direction) is then found and shown in Figs. 7–10. It can be observed from the figures that thermal disturbance force F_Q induces additional transverse displacement in the distributed control system. The magnitude of displacement will naturally vary depending on the strength of heat flux. The heating (cooling) effects will be even more for the large control systems having large PVDF layers due to their large exposure areas to the heating (cooling). To check the validity of the FEM modeling of the thermal field as developed earlier, the temperature increase in the PVDF actuator layer at the tip θ_1 due the heat flux of 5 kW/m^2 is found and shown in Fig. 11. The steady-state value of θ_1 is compared with the result obtained by the elementary heat conduction equation in z direction given by

$$q = k_3 \theta_1 / L \quad (35)$$

where $q = 5000 \text{ W/m}^2$, $k_3 = 0.12 \text{ W/Km}$, and $L = 0.0001 \text{ m}$. From Eq. (35), θ_1 is found to be 4.17 K , which checks with the steady-state value of θ_1 in Fig. 11.

Note that the results obtained with another piezoelectric material, PZT-5, showed thermal effects similar to those of PVDF. Piezoelectric properties of PZT-5 can be found in Ref. 28. Hence, the inclusion of thermal effects is concluded to be important in the precision distributed control of advanced intelligent structures. Note that because the control applications require more power with the increasing performance and precision requirements, a thermal disturbance force caused by Q whose strength is around 5 kW at each node will always be present due to the feedback voltage. For example, if the feedback voltage at the i th node is 1500 V , then the heat generated at the i th node will be $Q_i = V_i^2/R = 1500^2/500 \text{ W} = 4.5 \text{ kW}$. When an independent heat source (or sink) is present in the environment where the control system is to operate,

its thermal effects will add to the already present thermal effects induced by the feedback voltage.

V. Conclusion

A finite element formulation is presented for thermopiezoelectric materials, and its application to integrated sensing and control of intelligent structures is discussed. The distributed vibration sensing and control of a piezoelectric bimorph finger and a beam are considered in the numerical investigation.

Large space structures used in space applications are vulnerable to dynamic excitations caused by the slewing/pointing maneuvers and various onboard activities. The precision sensing and control aspects, including thermal disturbance monitoring and rejection in thermally adverse environments, are important for the safe and effective operation of these structures. If the piezoelectric material is sensitive to the temperature changes, the inclusion of thermal effects may become even more important in the distributed precision sensing and control of these structures.

It is evident from the foregoing discussion and numerical results that thermal effects will have an impact on the performance of a distributed control system. The degree of impact may vary depending on the piezoelectric material, the environment where the system operates, and the magnitude of the feedback voltage. In some cases as stated earlier, it may be impossible to accurately design a distributed control system without including the thermal field. Thus, the development of distributed thermopiezoelectric sensors and actuators is expected to be essential in the design of future lightweight, high-performance structures with intelligent adaptive capabilities.

References

- Curie, J. and Curie, P., *Comptes Rendus*, Vol. 91, 1880, pp. 294–295.
- Forward, R. L., "Electronic Damping of Vibrations in Optical Structures," *Journal of Applied Optics*, Vol. 18, No. 5, 1979, pp. 690–697.

- ³Bailey, T., and Hubbard, J. E., "Distributed Piezoelectric-Polymer Active Vibration Control of a Cantilever Beam," *Journal of Guidance, Control, and Dynamics*, Vol. 8, No. 5, 1985, pp. 605–611.
- ⁴Hagood, N. W., Chung, W. H., and von Flotow, A., "Modelling of Piezoelectric Actuator Dynamics for Active Structural Control," *Proceedings of the AIAA/ASME/ASCE/AHS/ASC 31st Structures, Structural Dynamics, and Materials Conference* (Long Beach, CA), AIAA, Washington, DC, April 2–4, 1990, pp. 2242–2256.
- ⁵Hanagud, S., Obal, M. W., and Calise, A. J., "Optimal Vibration Control by the Use of Piezoelectric Sensors and Actuators," *Proceedings of the AIAA/ASME/ASCE/AHS/ASC 28th Structures, Structural Dynamics and Materials Conference* (Monterey, CA) AIAA, Washington, DC, April 6–8, 1987, pp. 987–997.
- ⁶Crawley, E. F., and de Luis, J., "Use of Piezoelectric Actuators as Elements of Intelligent Structures," *AIAA Journal*, Vol. 25, No. 10, 1987, pp. 2000–2010.
- ⁷Cudney, H. H., Inman, D. J., and Oshman, Y., "Distributed Structural Control Using Multilayered Piezoelectric Actuators," *Proceedings of the AIAA/ASME/ASCE/AHS/ASC 31st Structures, Structural Dynamics, and Materials Conference* (Long Beach, CA), AIAA, Washington, DC, April 2–4, 1990, pp. 2257–2264.
- ⁸Dimitriadis, E. K., Fuller, C. R., and Rogers, C. A., "Piezoelectric Actuators for Distributed Vibration Excitation of Thin Plates," *Journal of Vibration and Acoustics*, Vol. 113, No. 1, 1991, pp. 100–107.
- ⁹Jiang, Z. W., Chonan, S., Abe, H., and Tani, J., "Position Control of a Flexible Arm Using Piezoelectric Bimorph Cells," *Journal of Dynamic Systems, Measurement and Control*, Vol. 113, No. 2, 1991, pp. 327–329.
- ¹⁰Kawai, H., "The Piezoelectricity of Poly(vinylidene Fluoride)," *Japanese Journal of Applied Physics*, Vol. 8, No. 7, 1969, pp. 975–976.
- ¹¹Plump, J. M., Hubbard, J. E., and Bailey, T., "Nonlinear Control of a Distributed System: Simulation and Experimental Results," *Journal of Dynamic Systems, Measurement and Control*, Vol. 109, No. 2, 1987, pp. 133–139.
- ¹²Allik, H., and Hughes, T. J. R., "Finite Element Method for Piezoelectric Vibration," *International Journal for Numerical Methods in Engineering*, Vol. 2, No. 2, 1970, pp. 151–157.
- ¹³Nailon, M., Coursant, R. H., and Besnier, F., "Analysis of Piezoelectric Structures by a Finite Element Method," *ACTA Electronica*, Vol. 25, No. 4, 1983, pp. 341–362.
- ¹⁴Tzou, H. S., and Tseng, C. I., "Distributed Piezoelectric Sensor/Actuator Design for Dynamic Measurement/Control of Distributed Parameter Systems: A Piezoelectric Finite Element Approach," *Journal of Sound and Vibration*, Vol. 137, No. 1, 1990, pp. 1–18.
- ¹⁵Mindlin, R. D., "On the Equations of Motion of Piezoelectric Crystals," *Problems of Continuum Mechanics*, edited by J. Radok, SIAM, Philadelphia, PA, 1961, pp. 282–290.
- ¹⁶Mindlin, R. D., "Equations of High Frequency Vibrations of Thermopiezoelectric Crystal Plates," *International Journal of Solids and Structures*, Vol. 10, No. 6, 1974, pp. 625–637.
- ¹⁷Nowacki, W., "Some General Theorems of Thermopiezoelectricity," *Journal of Thermal Stresses*, Vol. 1, No. 2, 1978, pp. 171–182.
- ¹⁸Jesan, D., "On Some Theorems in Thermopiezoelectricity," *Journal of Thermal Stresses*, Vol. 12, No. 2, 1989, pp. 209–223.
- ¹⁹Rogers, C. A., and Barker, D. K., "Experimental Studies of Active Strain Energy Tuning of Adaptive Composites," *Proceedings of the AIAA/ASME/ASCE/AHS/ASC 31st Structures, Structural Dynamics, and Materials Conference* (Long Beach, CA), AIAA, Washington, DC, April 2–4, 1990, pp. 2234–2241.
- ²⁰Hilczer, B., and Malecki, J., *Electrets*, Elsevier, New York, 1986, Chap. 8.
- ²¹Guyan, R. J., "Reduction of Stiffness and Mass Matrices," *AIAA Journal*, Vol. 3, No. 2, 1965, p. 380.
- ²²Tzou, H. S., "Development of a Light-Weight Robot End-Effector Using Polymeric Piezoelectric Bimorph," *Proceedings of the 1989 IEEE International Conference on Robotics and Automation* (Scottsdale, AZ), Computer Society Press, Los Angeles, CA, May 14–19, 1989, pp. 1704–1709.
- ²³Lee, W. K., and Choy, C. L., "Heat Capacity of Fluoropolymers," *Journal of Polymer Science: Polymer Physics Edition*, Vol. 13, No. 3, 1975, pp. 619–635.
- ²⁴Choy, C. L., Chen, F. C., and Luk, W. H., "Thermal Conductivity of Oriented Crystalline Polymers," *Journal of Polymer Science: Polymer Physics Edition*, Vol. 18, No. 6, 1980, pp. 1187–1207.
- ²⁵Choy, C. L., Chen, F. C., and Young, K., "Negative Thermal Expansion in Oriented Crystalline Polymers," *Journal of Polymer Science: Polymer Physics Edition*, Vol. 19, No. 2, 1981, pp. 335–352.
- ²⁶Sessler, G. M., "Piezoelectricity in Polyvinylidene fluoride," *The Journal of the Acoustical Society of America*, Vol. 20, No. 6, 1981, pp. 1596–1608.
- ²⁷Tzou, H. S., and Zhong, J. P., "Adaptive Piezoelectric Shell Structures: Theory and Experiments," *Proceedings of the AIAA/ASME/ASCE/AHS/ASC 32nd Structures, Structural Dynamics, and Materials Conference* (Baltimore, MD), AIAA, Washington, DC, April 8–10, 1991, pp. 2290–2296.
- ²⁸Berlincourt, D. A., Curran, D. R., and Jaffe, H., "Piezoelectric and Piezomagnetic Materials and Their Function in Transducers," *Physical Acoustics*, edited by Warren P. Mason, Vol. 1, Pt. A, Academic Press, New York, 1964, pp. 170–267.